Biomass Conversion and Biorefinery
https://doi.org/10.1007/s13399-023-04961-9

ORIGINAL ARTICLE

Fioria vitifolia Linn. leaf extract-derived Zinc oxide nanoparticles: green synthesis, characterization and its biological activities

Raji Meena[1] · Sivakumar Saipraba[1] · Devarajan Natarajan[2] · Abdel-Rhman Z. Gaafar[3] · Irshad Arshad[4] · Subban Murugesan[1]

Received: 4 July 2023 / Revised: 27 September 2023 / Accepted: 28 September 2023

Abstract
In this study, Zinc oxide nanoparticles (ZnO NPs) were efficiently synthesized using *Fioria vitifolia* leaf extracts. These NPs were then examined using techniques such as scanning electron microscopy (SEM) with electron diffraction X-ray spectroscopy (EDX), Fourier transform infrared spectrum (FTIR), X-ray diffraction (XRD), and transmission electron microscopy (TEM). Ultraviolet–visible spectrum (UV) of ZnO NPs shows a distinctive absorbance region around 371 nm. FTIR spectrum investigation could have shown functional groups of amino acids and peptides that act as stabilizing agents. The hexagonal wurtzite structure has been confirmed via powder XRD signals. Additionally, Electron microscopy analysis of the ZnO NPs demonstrates their sphere-shaped form, and EDX spectra show their chemical composition. In vitro testing is performed on green ZnO NPs to see whether they have the ability to inhibit both Gram + ve (*Bacillus subtilis* and *Staphylococcus aureus*) and Gram -ve (*Klebsiella pneumonia* and *Escherichia coli*) bacterium varieties. By two distinct approaches, ABTS (2,2-azino-bis-3-ethylbenzothiazoline-6-sulphonic acid) IC_{50} value is 3.07 µg/ mL and DPPH (2,2′-diphenyl1-picrylhydrazyl) IC_{50} value is 122.37 µg/ mL, ZnO NPs shows good antioxidant potential. Human red blood cell membrane stabilization (HRBC) IC_{50} value was 60.95 µg/ mL and the albumin denaturation test IC_{50} value was 275 µg/ mL, indicating ZnO NPs have a significant anti-inflammatory effect. Using MTT colorimetric assay, the liver cancer (HepG2) cell line was assessed, and the IC_{50} value was discovered to be 52.60 µg/ mL. Based on the findings, the synthesized ZnO NPs using *Fioria vitifolia* are recommended that nano-based medications be created in the future.

Keywords ZnO · HepG2 cell line · *Fioria vitifolia* extract · Antibacterial · Antioxidant · Anti-inflammatory

1 Introduction

Due to its myriad potential applications in catalytic processes, detecting, gadgets, imaging, and medicine, scientists have recently been increasingly interested in creating NPs. An innate capacity of living things to decrease metallic components has been acknowledged by scientists since the nineteenth century, but the method is still a mystery. Researchers are increasingly focusing on biological methods as a result of the efficacy of generating NPs using biological suppression, capping, and strengthening factors while eliminating hazardous substances and a surplus of energy [1].

NPs with dimensions that fluctuate between one to one hundred nanometre can provide the connection between massive substances and nuclear or complex molecules [2]. NPs are being developed all over the world as a result of a variety of intriguing and unique characteristics that enable their use in a variety of logically unrelated fields, including luminescence photocatalytic potential and photodiode response on the one hand and nano-diagnostics, nanomedicine, and antimicrobials on the other [3].

The most versatile of them, dating back to the Bronze Age, are ZnO nanoparticles. They have attracted the interest of researchers due to their unusual visual and chemical-based

✉ Subban Murugesan
drsmbtjas@periyaruniversity.ac.in

[1] Department of Botany, Periyar University, Salem-636011, Tamil Nadu, India

[2] Department of Biotechnology, Periyar University, Salem-636011, Tamil Nadu, India

[3] Department of Botany and Microbiology, College of Science, King Saud University, P.O. Box 11451, Riyadh, Saudi Arabia

[4] The Department of Biology, New Mexico Highlands University, Las Vegas, NM 87701, USA

Published online: 17 October 2023

actions, and their ability to be readily impacted by altering the shape, and they garnered considerably greater attention in the scientific sector [4].

Zinc oxide, an inorganic powder that is durable and resistant to severe procedures compared to organic materials, offers a possible substitute for chemical preservatives with microbicidal capabilities. ZnO is regarded as one of the GRAS (generally acknowledged as safe) elements for use in humans [5]. The potential biological applications of ZnO NPs are increased by their ease of production, non-toxicity, environmental friendliness, biocompatibility, and biosafety [6]. Due to its unique optical and chemical behavior, which may be readily improved by modifying their size and shape, ZnO NPs have been considerably garnering the attention of researchers among other NPs. In addition, the ZnO NPs are renowned for their photo-catalytic and photo-oxidizing abilities for chemical and biological species. In the fields of medicine and environmental science, ZnO NPs are used as antimicrobial, anti-inflammatory, anti-diabetic and as a photocatalytic agent for the degradation of organic pollutants responsible for water pollution due to their distinctive catalytic and oxidizing abilities [7]. ZnO NPs are essential for several biological applications, including their anti-angiogenic, anti-tumor, wound-healing, UV scattering, and wound-healing capabilities. In commercial products like paints and cosmetics, ZnO NPs play a crucial role [8].

Agriculture is the backbone of the economies of developing countries, this sector is facing numerous global challenges like climate change, urbanization, sustainable resource use, and environmental problems like runoff, and accumulation of fertilizers and pesticides. Food demand is expected to increase with population increase from 6 billion people to 9 billion people by the year 2050. Consequently, we need to use efficient methods to improve the sustainability of agriculture [9]. Agriculture and food production are being revolutionized by nanotechnology. Nanotechnology's use in agriculture is attracting interest due to its effectiveness in the exact control and release of fertilizers, insecticides, and herbicides. The development of nano-sensors can aid in calculating the necessary dosage of agricultural inputs like fertilizers and insecticides [10]. High sensitivity, minimal detection limits, extreme selectivity, quick reactions, and compact diameters are all features of nano-sensors used to detect pesticide residue. They can also measure the amount of soil moisture and nutrients. Nano-fertilizers can be quickly absorbed by the plants. Slow-release fertilizers that are nano-encapsulated can reduce environmental pollution and fertilizer usage [11].

In the past, leaf extracts of *Salvia officinalis*, *Parthenium hysterophorus*, and *Solanum torvum*, as well as others, have been utilized to create ZnO NPs using a green synthesis process [12–14]. Since the extracts aid in creating well-organized ZnO NPs and increase their antibacterial activity while also serving as reducing and stabilizing agents, using green methods has several advantages [15]. Due to its uniqueness and well-known therapeutic characteristics, *Fioria vitifolia* was taken into consideration for developing ZnO NPs.

The plant *Fioria vitifolia* Linn., a native of India and a member of the Malvaceae family, proceeds by the name *Hibiscus vitifolius*. Pain relieving, inflammatory-fighting properties, reducing fever, urinary tract infection, unpleasant, cerebral depressant, antibacterial, and anti-fertility effects are present in the herb in its traditional use. In herbal therapy, plant extracts have been reported as a remedy for alleviating pain, fever, and inflammation. The pharmacological effect of plant (rat studies) showed very effective than aspirin drug [16].

Considering the above facts, in the present study, *Fioria vitifolia* leaf extracts were successfully used to synthesize zinc oxide NPs. To define and validate the green production of NPs, many spectroscopic and microscopic investigations, such as ultraviolet–visible spectroscopy, the FTIR technique, HR-TEM, XRD analysis, and scanning electron microscope with energy-dispersive X-ray spectroscopy, have been examined. The biological (antioxidant, antibacterial, anti-inflammatory, and anticancer) characteristics of ZnO NPs from *Fioria vitifolia* were also tested in vitro.

2 Experimental section

2.1 Chemicals and reagents

Zinc acetate dihydrate [Zn $(CH_3COO)_2$. $2H_2O$], sodium hydroxide pellets, ethanol, methanol, DPPH (2,2-diphenyl-1-picrylhydrazyl), and ABTS (2,2-azino-bis-3-ethylbenzothiazoline-6-sulphonic acid) were acquired from HiMedia laboratories, Mumbai, India, and used as received. All other reagents were of an analytical grade.

2.2 The strategy of creating a water-based Fioria vitifolia extract from leaves

The foliage of *Fioria vitifolia* was washed under fresh water, regularly rinsed with distilled water, and then desiccated for ten days in a shaded environment to wring out any wet matter that could have remained [17]. The leaves were pulverized into a homogeneous, finely ground powder using an electric blender in a monitored laboratory setting

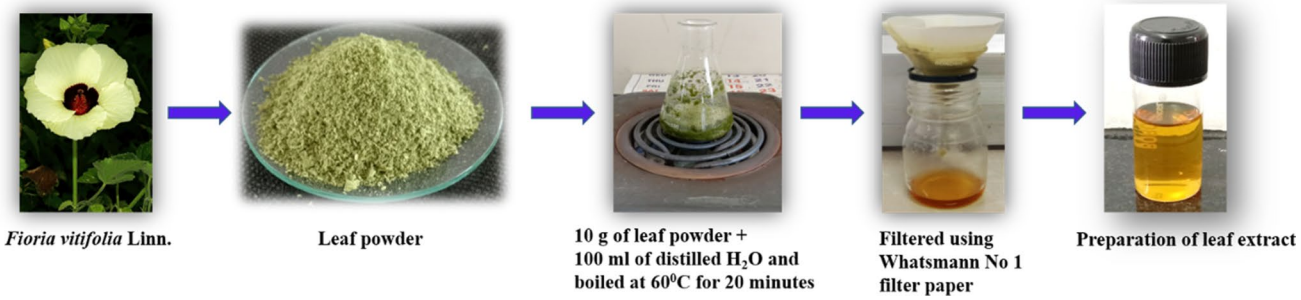

Fig. 1 Schematic diagram shows the preparation of leaf extract

[18]. To filter the mixture through Whatman No 1 filter paper, hundred milliliters of purified water and 10 g of powdered leaves were mixed, heated at 60 °C for a period of twenty minutes, and then allowed to cool to room temperature (Fig. 1).

2.3 ZnO NPs made using a green method

Tiny particles of zinc oxide were synthesized with an altered version used by [19] using plant resources. NPs were created using Zinc acetate as an initial substance. 50 mL aqueous solution of 2 M Zinc acetate was prepared using deionized water. pH was then adjusted to 12 by adding extracts of foliage (5 mL) and two molar sodium hydroxide (50 mL) after 2 h of stirring. To get rid of contaminants, the white precipitate was washed multiple times with purified water and then ethanol (C_2H_5OH). The resulting product was then drenched at 60 °C in an oven, and the tiny particles were subsequently calcined for 3 h at 350 °C in a muffle furnace. These operations are shown in Fig. 2.

3 Characterization techniques

3.1 UV–spectrum analysis

Using a UV–Vis spectroscopic analysis of tiny particles of zinc oxide, the spectral characteristics of the created nanomaterial were investigated. After only a small quantity of

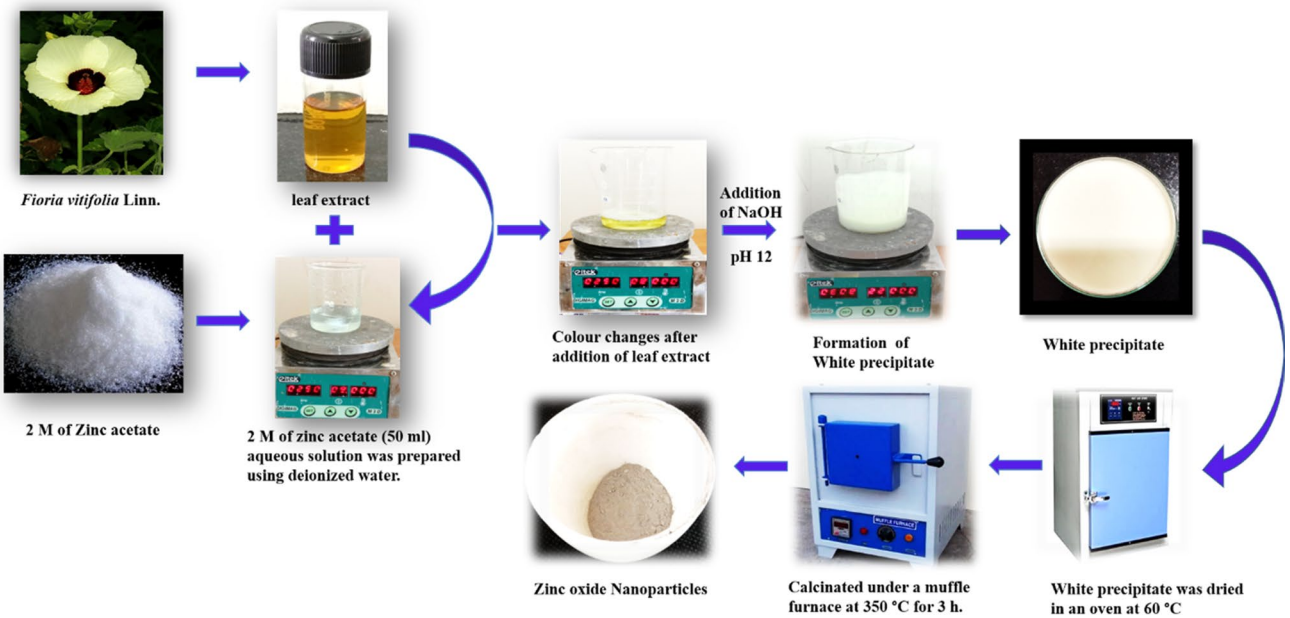

Fig. 2 Schematic diagram shows the synthesis of zinc oxide nanoparticles using the leaf extract of *Fioria vitifolia* Linn

the nano-powder was reincorporated in around 10 mL of distilled water and read over 200 and 800 wavelength, the maximum absorbance was determined using a Shimadzu UV-1800 UV-Spectrophotometer [20].

3.2 FT-IR analysis

We employed powder XRD and FT-IR to investigate the molecular makeup, content, configuration, and dimension of the NPs. The sample's Fourier-transform infrared spectroscopy adsorption spectrum was recorded on a Perkin Elmer's (Model; 95,277) FT-IR imaging Spectrometer Rainbow Spectrum RX-1 in the wavelength range of 4000–400 cm^{-1} [21].

3.3 Analysis of X-ray powder diffraction (XRD)

The structure of the crystals and the high purity of naturally synthesized zinc oxide NPs have been investigated using an XRD (XRD 7000, Shimadzu, Japan) system with Copper K-alpha (1.541 A°) exposure and a Ni filter functioning at an input voltage of fifty kV and a current of thirty mA [22].

3.4 Analysis employing SEM alongside EDX and TEM

The surface characteristics and elemental makeup of the manufactured nanomaterial were examined using SEM alongside EDX (Make: EVO18, Carl Zeiss Microscopy, USA). Using a concentrated electron source from a charged particle cannon and a 15 kV acceleration voltage, the sample was scanned to provide a highly accurate planar picture [23]. The grain size of the ZnO NPs was assessed using a 200 keV electron source and an FEI Tecnai T20 transmission electron microscope [24].

4 Biological activity

4.1 Antibacterial properties

The synthesized NPs made of ZnO have been evaluated for their ability to kill bacteria by an agar disc diffusion technique that causes sickness in humans such as *Bacillus subtilis*, *Staphylococcus aureus*, *Klebsiella pneumonia*, and *Escherichia coli*. The overnight fresh culture of each strain was swabbed uniformly onto its plate. The impregnated ZnO NPs solution in volumes of 25, 50, and 75 µL was placed on the plates and heated to 37 °C for 24 h. As a benchmark, commercial antibiotic discs were employed. The extent of zonation's development around the disc was evaluated after an appropriate incubation period [25].

4.2 *In vitro* antioxidant assay

4.2.1 Test for DPPH radical sequestration

The method used to quantify samples' total capacity to eliminate free radicals (as evaluated by the DPPH radical test) was somewhat modified from that employed previously by [26]. Methanol was utilized to prepare 500 µM of DPPH. The reaction mixture for the DPPH scavenging test is made up of 1 mL of ethanol, 100 µL of DPPH solution, and different extract concentrations. For 5 h in complete darkness at 23 °C, the reaction product was left to sit. The preparations' ability to capacity to neutralize harmful radicals is demonstrated by the disappearance of the original purple tint. The absorbance of the resultant substance was calculated at 517 nm.

$$\text{Scavenging activity (\%)} = [\text{absorbance (control)} - \text{absorbance (sample)} / \text{absorbance (control)}] \times 100.$$

4.2.2 Radical scavenging test for ABTS

The ABTS neutralizing experiment was conducted via a modification of [27] methodology. Water was used to dissolve 7 mM of ABTS. The ABTS radical cation (ABTS● +) was created by reacting the ABTS base suspension with 2.45 mM Potassium persulfate ($K_2S_2O_8$) final concentration, which then remained undisturbed at ambient level for 12 to 16 h before usage. To achieve equilibrium at 30 °C and an absorption value of 0.70 at 734 nm, the resulting mixture was mixed with C_2H_5OH.

For the ABTS scavenging test, the reaction mixture consisted of 900 µl of ABTS solution, and various extract concentrations, and the solution was mixed with C_2H_5OH to 1 mL. Three hours were endured incubation, the reaction mixture at room temperature without any illumination. The extracts' ability to scavenge free radicals was shown by the loss of the original blue hue. At a wavelength of 734 nm, the absorbing capacity of the reaction mixture was assessed.

$$\text{Scavenging activity (\%)} = [\text{absorbance (control)} - \text{absorbance (sample)} / \text{absorbance (control)}] \times 100.$$

4.3 An anti-inflammatory response

4.3.1 Method for stabilizing HRBC membrane

The effectiveness of the sample in laboratory anti-inflammatory properties was evaluated using the HRBC barrier stabilization technique [28]. Healthy participants who had avoided NSAIDS for 2 weeks before, to the study had their blood collected. The collected blood was combined with a comparable volume of sterile Alsever solution (2% glucose, 0.8% sodium citrate, 0.5% citric acid, and 0.42% sodium chloride in water). After packed cells were rinsed with 0.85% iso-saline (with a pH of 7.2), and the blood was centrifuged at 3000 revolutions per minute, an iso-saline solution of 10% (v/v) was produced. The test combination contains samples with a variety of sample concentrations, as well as 0.5 mL of HRBC solution, 1 mL of phosphate buffer (0.15 molar, pH 7.4), and 2 mL of hyposaline (0.36%). As a benchmark medication, diclofenac was employed. The hyposaline solution was replaced in the control with 2 mL of purified water (H_2O). All of the test solutions were centrifuged after 30 min of 37° C incubation. At 560 nm, a spectrophotometer was used to quantify the amount of hemoglobin in the supernatant solution. To calculate the percentage of haemolysis, it was assumed that all haemolysis that occurs in the presence of purified H_2O would be 100%.

$$\text{Anti} - \text{inflammatory activity } (\%) = [\text{absorbance (control)} - \text{absorbance (sample)} / \text{absorbance (control)}] \times 100.$$

4.3.2 Albumin denaturation assay suppression

The soothing effect of the nanomaterial was investigated by using the prevention of denaturation of bovine serum albumin, the same as in the prior approach described by [29]. After adding different test chemical concentrations to 450 µL of 0.5% bovine serum albumin, purified H_2O was used to prepare the solution up to 1 mL. The resultant solution was raised to 37 °C for a period of 20 min. Albumin-denatured state was achieved after incubation by holding the product at 72 °C over 15 min. After freezing the reaction liquid, 2.5 mL of a 0.2 M buffer solution of trisodium phosphate (pH 6.3) was added. The turbidity was measured at 660 nm using an Epoch 2 UV–visible multi-well plate reader (Biotek, USA). The lone buffer was used to set a blank. In the absence of bovine albumin, true blanks were established using test chemicals at the same concentration utilized in the experiment. The percentage inhibition of protein denaturation obtained by:

$$\text{Anti} - \text{inflammatory activity } (\%) = [\text{absorbance (control)} - \text{absorbance (sample)} / \text{absorbance (control)}] \times 100.$$

4.4 Action against cancer

4.4.1 The preservation of a cancerous cell line

National Centre for Cell Science, Pune, supplied several carcinoma cell lines (colon tumor (HT 29), malignancy of the liver (HepG2), and prostate cancer (MCF 7)), which were cultured in α-MEM (Minimum Essential Medium Eagle, alpha modification) containing 10% fetal bovine serum. The cells were maintained at 370 °C, 5% CO_2, 95% air, and 100% relative humidity. Every week, maintenance cultures were passed, and the growth media was switched out two times weekly.

4.4.2 Method of cell therapy

The single-walled cells were divided into individual cell suspensions using Ethylenediaminetetraacetic acid (EDTA), and alive cells were measured by a haemocytometer. Each of the cell suspensions was reduced to a final density of 1×105 cells per mL using a medium containing 5% fetal bovine serum (FBS). Using a hundred microliters of cell solution per well, 10,000 cells were seeded onto plates with 96 wells. The cells were then given time to adhere over an incubation period at 37C, 5% of carbon dioxide, 95% of air, and a humidity level of 100%. After 24 h, the test samples were subjected to increasing doses of the cells. They were first dissolved in Dimethyl sulfoxide, and a sample preparation was then mixed with seraless solution to double the required final highest assay dosage. Four further consecutive dilutions were carried out to produce an overall 5 sample dosage. The requisite final material concentrations were achieved by adding these varied sample dilutions in aliquots of 100 µl to the relevant wells that already had 100 µl of the medium. The plates were then incubated for a further 48 h at 37 °C, 5% of carbon dioxide, 95% of air, and a humidity level of 100% after the sample had been added. Every dosage was maintained in triplicate, and the media without any samples served as the control [30].

4.4.3 MTT assay

The yellow tetrazolium salt MTT is hydrophilic. The mitochondrial enzyme succinate-dehydrogenase breaks

the tetrazolium ring of the MTT and transforms the formazan into an insoluble purple material. As a result, the number of cells that are alive closely relates to the amount of Formazon generated. Each well received 15 µL of MTT (5 mg/mL) in PBS (phosphate buffered saline) 48 h after the first incubation, and then underwent a 4-h incubation at 37 °C. After removing the MTT medium, 100 µL of Dimethyl sulfoxide was added for dissolving the Formazon crystals that had formed. A microplate reader was then used to determine the absorbance of the material at 570 nm [31].

4.5 Analytical statistics

The data was examined by employing the one-path ANOVA method using the data analysis program Statistical Package for the Social Sciences (SPSS version 21, IBM Corporation, Armonk, New York, America). At $p < 0.05$, the variance was deemed significant.

5 Results and discussion

5.1 Characterization of ZnO NPs

5.1.1 Evaluation of the ultraviolet spectrum and band gap energy

The primary tool for assessing the confirmation of the synthesized nanomaterial is the UV–visible absorption spectrum. The white precipitate that forms when Zinc acetate is added to the extract is one of the most important signs of the production of ZnO NPs. Between 200 and 800 wavelength, the ZnO NPs frequently exhibit a broad peak. [32] claim that ZnO NPs with a prominent absorbance peak at 371 nm were produced using *Fioria vitifolia* leaf extract (Fig. 3a). Previous research has indicated that ZnO NPs exist because the ultraviolet–visible spectrum exhibits a significant absorbance peak at 371 nm [33]. Similar to this, [34] pointed out that the identification of an absorption peak at 371 nm in the ultraviolet spectrum offered unmistakable proof for the production of ZnO NPs.

The band gap energy value of synthesized ZnO NPs from *Fioria vitifolia* was found with the help of the Tauc plot equation.

$$(\alpha h\upsilon)^2 = A(h\upsilon - Eg)$$

whereas hυ is the energy of the incident photon, αA is the absorption coefficient, Eg is the optical band gap energy, and the exponent n depends on the type of transition between bands. Since a direct transition is considered for ZnO, $n = 2$ for our estimations [35]. The plot of (αhυ) 2 versus (hυ) is shown in Fig. 3b. The band gap energy value for ZnO NPs was estimated to be 3.31 eV.

5.1.2 Analysis of Fourier transform infrared spectrum

By FTIR research, the potential functional groups involved in the formation of NPs made of ZnO were found. Figure 4 displays the FT-IR spectrum of ZnO NPs between 500 and 4000 cm^{-1}. The -OH stretching

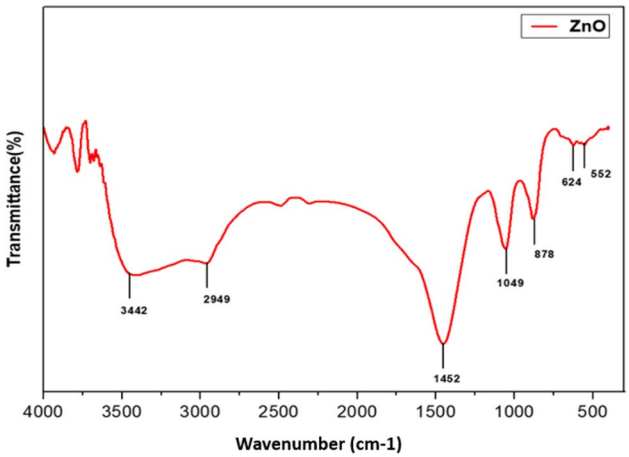

Fig. 4 FTIR spectrum of ZnO NPs synthesized by *Fioria vitifolia*

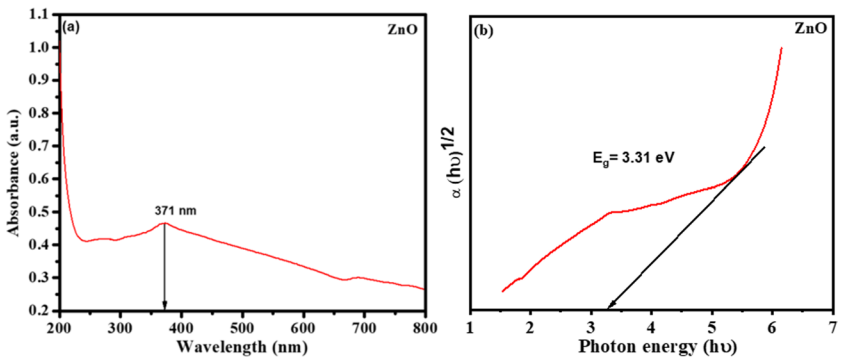

Fig. 3 **a** UV- vis absorption spectrum. **b** Tauc plot of ZnO NPs synthesized using *Fioria vitifolia*

Table 1 FTIR functional groups analysis for *Fioria vitifolia* ZnO NPs

S. no	Wavenumber(cm^{-1})	Bond source	Functional group	Peak description
1.	3442	O–H stretch	Alcohols, Phenol	strong, broad
2.	2949	C–H stretch	Alkanes	Medium
3.	1452	C–H bend	Alkanes	Medium
4.	1049	C–N stretch	Aliphatic amines	Medium
5.	878	C–H bend	1, 2-disubstituted	Strong
6.	624	C–Cl stretch	Halo compound	Strong
7.	552	C–I stretch	Halo compound	Strong

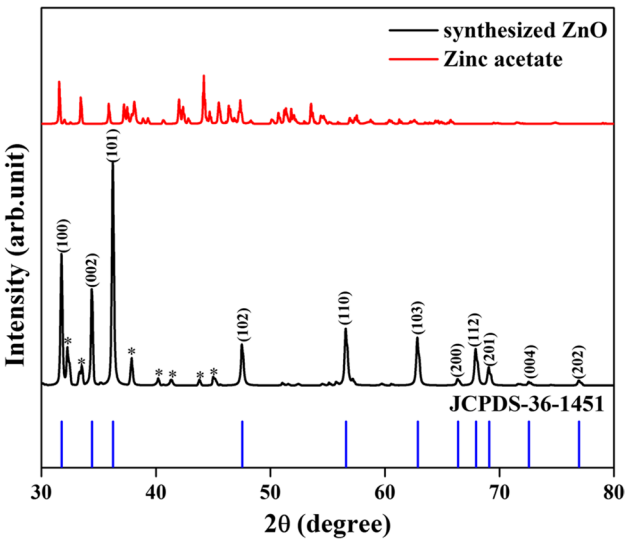

Fig. 5 X-ray diffraction spectrum of ZnO NPs synthesized using *Fioria vitifolia*

vibrations were detected due to the significant peak at 3442 cm^{-1}. The existence of C-H stretching was suggested by the medium peak, which was located in the vicinity of 2949 cm^{-1}. The peak at 1452 cm^{-1} is caused by a bend in the C–H bend [36]. The height of the peak at 1049 cm^{-1} is attributed by [37] to the C–N stretching vibration of the amine functional group. According to [38], the presence of the C–H bends in the alkane group causes a significant rise at 878 cm^{-1}. C–Cl stretching may be seen at the signal at 624 cm^{-1} [39]. The signal between 400 and 600 cm^{-1} is produced by bonding vibrations between zinc and oxygen. The strong bond is seen at 552 cm^{-1}, which is corroborated by the results of [40]. The current study displayed in Table 1, confirmed the formation of ZnO NPs. *Xanthomonas oryzae* pv. [41] and *Coleus aromaticus* [42] leaf extract were used in past studies on synthesized ZnO NPs to compare the current result to those findings.

5.1.3 Analysis of X-ray powder diffraction (XRD)

ZnO NPs that have been synthesized are examined using the XRD method to determine their crystal phases and crystallinity. Several Bragg reflections in ZnO NPs at 2θ values = 31.75°, 34.4°, 36.23°, 47.5°, 56.56°, 62.83°, 66.33°, 67.91°, 69.06°, 72.55°, and 76.93° indicate crystallographic axes of (100), (002), (101), (102), (110), (103), (200), (112), (201), (004), and (202) accordingly and other peaks (32.02°, 33.5°, 38.12°, 39.5°, 40.49°, 43.31°, and 45.49°) indicating * which are the impurities of Pure ZnO. Comparably, [43] published the XRD pattern of nanomaterial, and the current work demonstrates that all of the diffraction peaks (in Fig. 5) were accurately matched to the phase of hexagons (wurtzite pattern) of zinc oxide and are quite near to the approved values (Joint Committee on Powder Diffraction Standards (JCPDS) number. 36–1451). The average crystalline size of ZnO NPs was determined using Scherrer's Equation to be 26.1 nm.

5.1.4 Analysis of SEM (scanning electron microscopy) analysis employed with EDX (energy-dispersive X-ray spectroscopy)

SEM has been employed to look at the physical characteristics of nanoparticles. The agglomerated morphology of ZnO NPs which are produced from *Fioria vitifolia* leaf extract are depicted in Fig. 6A and B, a SEM image. This SEM result coincides with earlier observations that plant extracts from *Cochlospermum religiosa* [44] and *Papaver somniferum* [45] developed ZnO NPs. SEM result is in support of previous work noticed that agglomerated morphology of ZnO NPs [46].

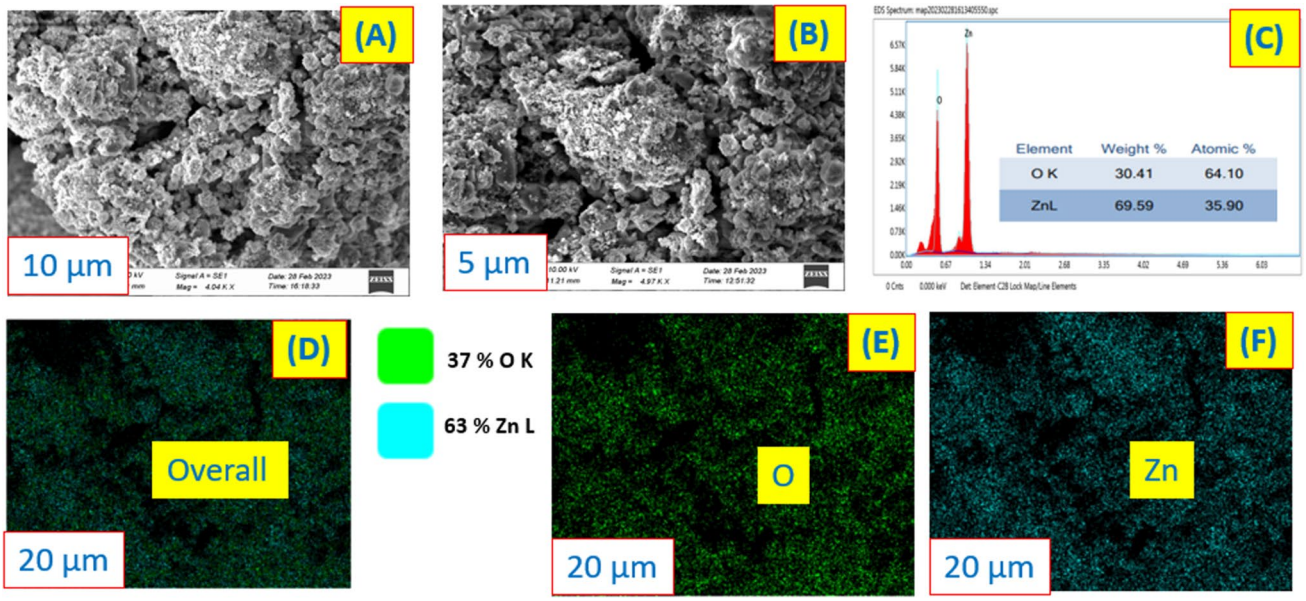

Fig. 6 **A**, **B**, **C**, **D**, **E**, and **F** SEM and EDX spectrum of synthesized ZnO nanoparticles from *Fioria vitifolia*

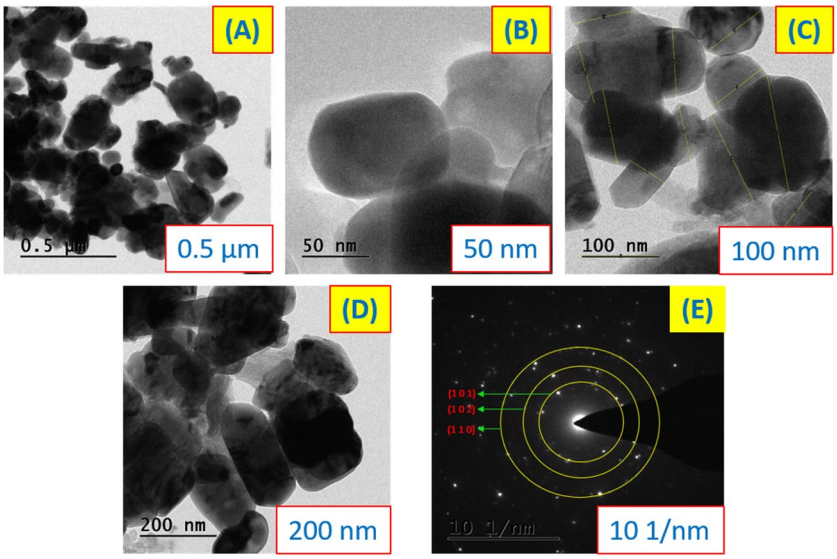

Fig. 7 **A**, **B**, **C**, **D**, and **E** TEM images and SAED pattern of ZnO NPs using *Fioria vitifolia*

The stereochemical makeup and mineral content of the NPs made of zinc oxide were analyzed by EDX (Fig. 6C, D, E, F); zinc and oxygen signals show that the synthesized nanocrystals were in their purest chemical state. O (37%), and Zn (63%), were the predominant elements in the obtained peaks [47]. While the previous study reported that zinc and oxygen were composed of 25% oxygen and 65% zinc, respectively, the EDX analysis in the current study shows similar results for synthesized NPs [48]. The present findings were matched with those made by zinc, which makes up more than 66.33% of the total constituents, and oxygen, which accounts for 25.48% and the results demonstrate that the high purity of the mediated ZnO NPs [49].

5.1.5 Analysis of TEM (transmission electron microscopy)

Transmission electron microscopy was employed to characterize the morphology of ZnO NPs, such as distribution of size, grain size, and nanoparticle dimensions. The spherical-shaped ZnO NPs made from *Fioria vitifolia* are described in SAED and TEM monographs. The average size of the ZnO NPs was found to be 88 nm. After TEM

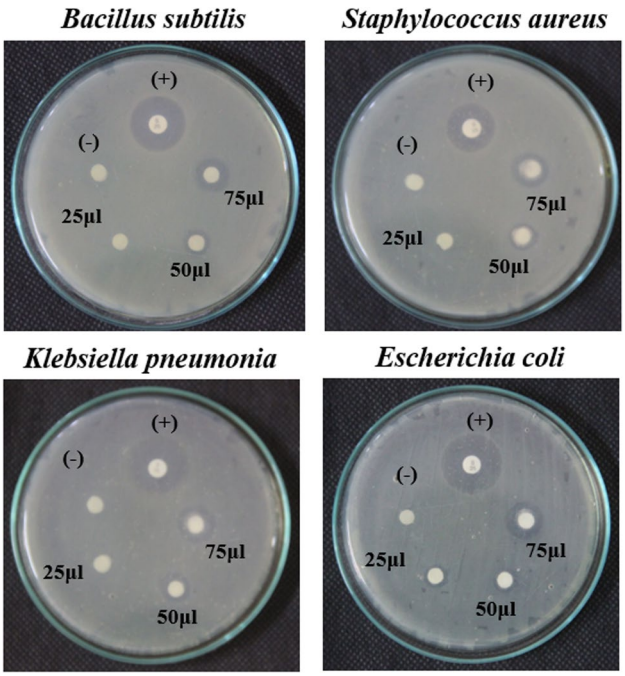

Fig. 8 Antibacterial activity of ZnO NPs against Gram-positive and Gram negative pathogens: (+) Positive control—Streptomycin (25 mcg). (−) Negative control—DMSO (25 µl)

analysis of the NPs, Fig. 7A, B, C, D, and E shows the SAED pattern that was found. SAED determined that (100), (002), and (101) were consistent and matched the XRD findings of [50]. Before this, [51] and [52] used TEM imaging examination of green-generated nanomaterials to show the random distribution of spherical-shaped nanomaterials.

5.2 Biological activity

5.2.1 Anti-bacterial resistance

The prepared particles made from ZnO demonstrated a substantial level of antibacterial capacity against common bacterial infections. Figures 8 and 9 display the disc-based diffusion approach for evaluating the antibacterial activity of various dosages of ZnO NPs (25, 50, and 75 µL), along with positive and negative controls made of Streptomycin discs (25 mcg) and DMSO (25 µL) respectively. *Bacillus subtilis* (11 ± 0.57 mm) had the most significant antibacterial zone of inhibition, followed by *Staphylococcus aureus* (10 ± 0.88 mm), *Klebsiella pneumonia* (10 ± 0.57 mm), and *Escherichia coli* (9 ± 0.33 mm). Table 2 displays the antibacterial zone of inhibition. The chosen infections don't exhibit a DMSO inhibition zone. Additionally, compared to the synthesized ZnO NPs Streptomycin had higher antibacterial activity. The current study found that Gram + ve bacteria had greater resistance to the bactericidal effects of synthesized ZnO NPs [53]. The findings demonstrated that

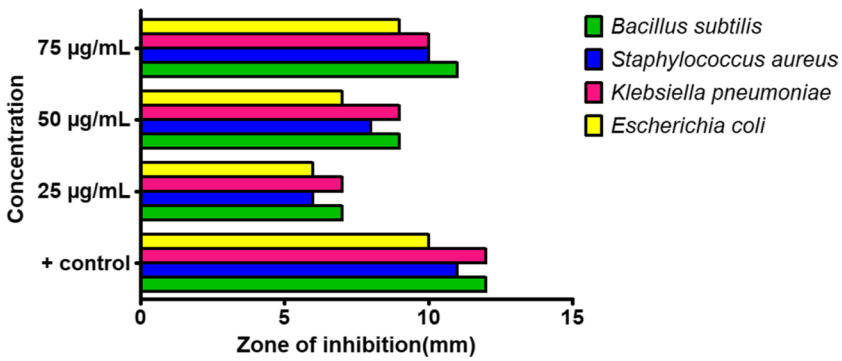

Fig. 9 Histogram of antibacterial activity of synthesized ZnO nanoparticles

Table 2 Antibacterial activity: zone of inhibition (ZOI) against Gram-positive and Gram-negative bacterial pathogens

S. no	Bacterial pathogens	Positive control – Streptomycin (25 mcg)	Negative control – DMSO (25 µL)	ZnO NPs		
				25 µL	50 µL	75 µL
1.	*Bacillus subtilis*	12 ± 0.57	-	7 ± 0.33	9 ± 0.33	11 ± 0.57
2.	*Staphylococcus aureus*	11 ± 0.57	-	6 ± 0.33	8 ± 0.88	10 ± 0.88
3.	*Klebsiella pneumoniae*	12 ± 0.57	-	7 ± 0.57	9 ± 0.88	10 ± 0.57
4.	*Escherichia coli*	10 ± 0.57	-	6 ± 0.33	7 ± 0.33	9 ± 0.33

Zone of inhibition measured as millimetre (mm) in diameter

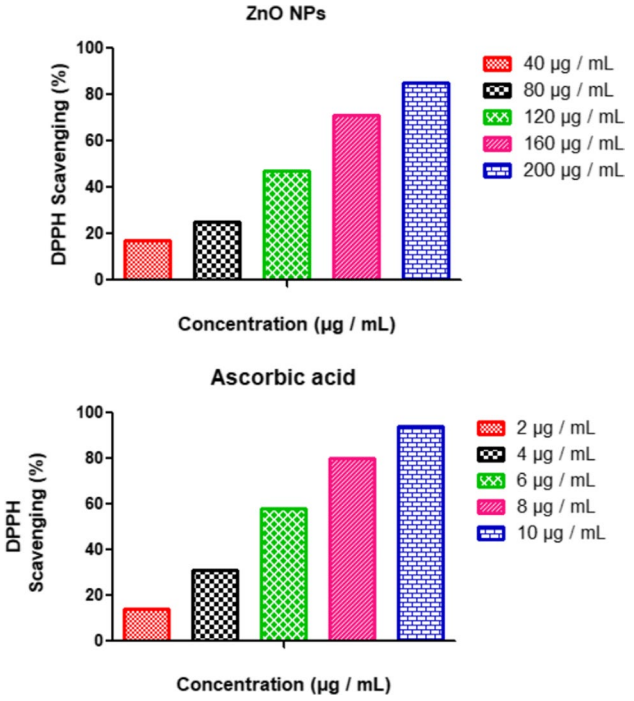

Fig. 10 Antioxidant activity of ZnO NPs at different concentrations by DDPH and ascorbic acid was used as a standard

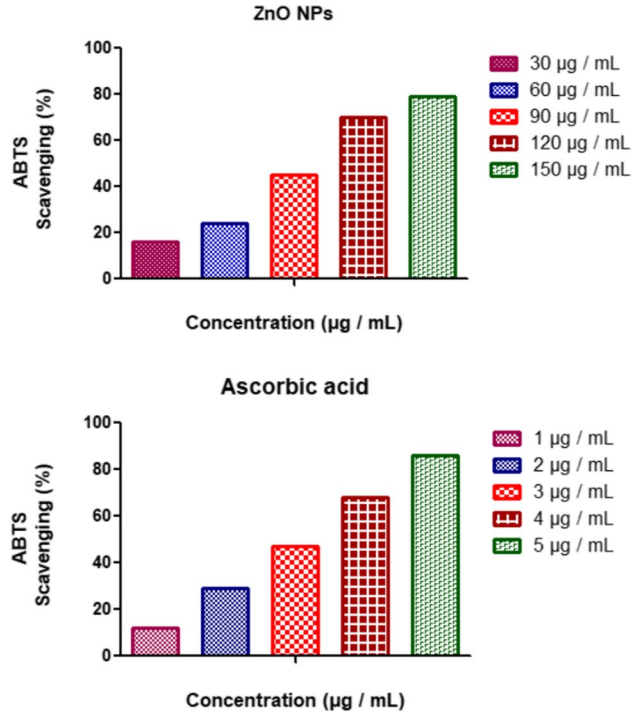

Fig. 11 Antioxidant activity of ZnO NPs at different concentrations by ABTS and ascorbic acid was used as a standard

Bacillus subtilis is the bacterial strain that is most sensitive to ZnO NPs inhibitory action, having the largest inhibition zone [54, 55].

5.2.2 *In vitro* antioxidant assay

Assay for scavenging DPPH radicals Using the DPPH technique, the antioxidant strength of synthetic NPs made of zinc oxide (purple hue changed to yellow) was evaluated. At 517 nm, this reduction was examined spectrophotometrically. The produced ZnO NPs of *Fioria vitifolia* leaves extract showed 16.5% inhibitory at a therapeutic level of 40 µg/ mL, and 85.2% at a dosage of 200 µg/ mL. The antioxidant activity of ZnO NPs, ascorbic acid, a standard compound, was found to have a value of 14.2% at 2 µg/ mL and 94.2% at 10 µg/ mL. The outcomes demonstrate ZnO NPs have the capacity to scavenge free radicals influenced by dose way. Figure 10 shows that NPs composed of ZnO have lower activity in neutralizing radicals than usual. To gauge the efficacy of an antioxidant activity, look at its IC_{50} value. The sample volume necessary to scavenge the free radicals by 50% is known as the IC_{50} value. The percent inhibition vs. concentration sigmoidal curve was used to calculate the IC_{50} values of ZnO NPs using a linear regression analysis. Compared to the benchmark value of 5.47 µg/ mL, the sample extract's IC_{50} value was much higher at 122.37 µg/ mL. As per the current study report the ZnO NPs have lesser antioxidant effectiveness than ascorbic acid and the outcome has been supported by [56]. The IC_{50} value of ZnO NPs is 134 µg/ mL, and prior findings of [57] were the complement of the present findings. Similar to this, [58] reported the free radical scavenging activity of DPPH using *Coccinia abyssinica* (Lam.) Cong. tuber extracts had an IC_{50} value of 127.74 µg/ mL.

ABTS radical scavenging assay Body cells and tissues produce free radicals, which are molecules or unpaired electrons. Additionally, called reactive oxygen species. In addition to internal variables like autoimmune disorders, external causes like inhaling nicotine, radiation, hazardous substances, and pollution, stress caused by oxidation may also occur from external sources like pollution, radiation, poisonous chemicals, and smoking. Numerous diseases are intimately related, including Parkinson's disease, arthritis, cancer, heart disease, and oxidative stress. By removing free radicals from our systems, antioxidants improve our bodies' levels of ROS. It halts tissue and cellular degeneration, including the degradation of proteins and DNA. Calculating the total antioxidant activity is done

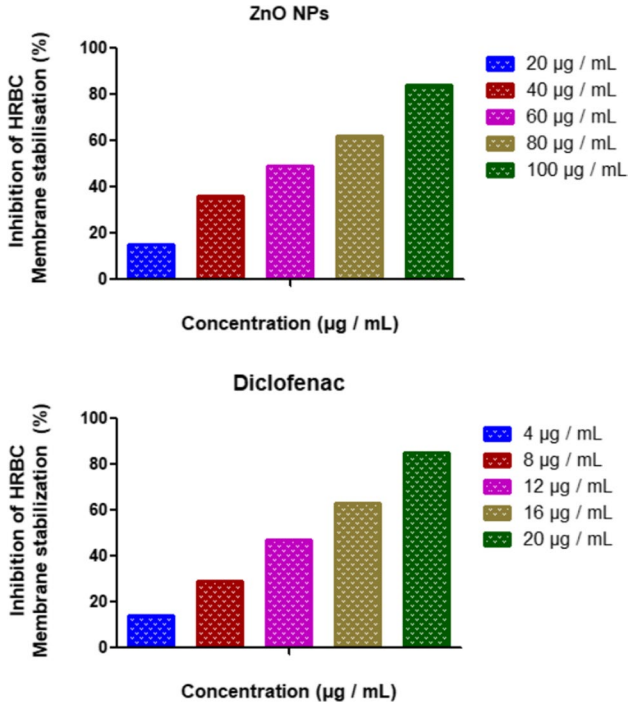

Fig. 12 Anti-inflammatory activity of ZnO NPs at different concentrations by HRBC membrane stabilization activity and diclofenac was used as a standard

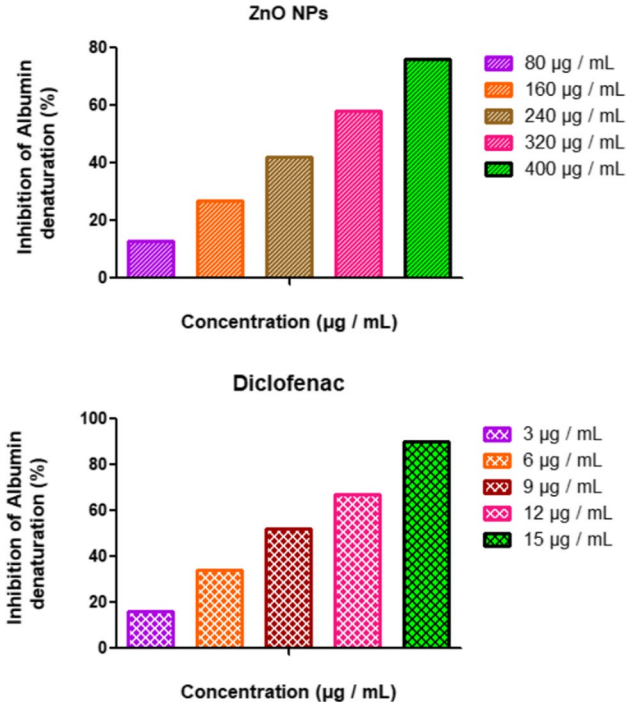

Fig. 13 Anti-inflammatory activity of ZnO NPs at different concentrations by albumin denaturation assay and Diclofenac was used as a standard

using a decolorization method known as the ABTS test. By decolorizing the response of a composed of persistent blue/green ABTS radical cations at 734 nm with various doses of ZnO NPs, the antioxidant capacity in the ABTS experiment was evaluated. To assess the relative antioxidant potential, standard ascorbic acid has been employed. In a dose-responsive way, the spherical-like ZnO NPs significantly acquired the radicals (30 to 150 µg/ mL); the highest extent of neutralizing capacity (79.2%) was reported at 150 µg/ mL dosage; the IC_{50} value for ZnO NPs is 95.52 µg/ mL. The dose of the standard (ascorbic acid) varied from 1 µg/ mL to 5 µg/ mL, and the concentration at which the highest percentage of scavenging potential (86.2%) was observed in Fig. 11 the IC_{50} value was 3.07 µg/ mL [59]. The results of this investigation agreed with a prior study by [60], and the highest free radical acts of scavenging of ABTS is 82.12%. Similarly, [61] reported the extreme scavenger behavior using the ZnO NPs as 89%.

5.2.3 *In vitro* anti-inflammatory activity of ZnO NPs

HRBC membrane stabilization test Inflammation is the living tissue's defense system against microbes, substances, bodily harm, toxins, destruction of tissue, etc. Lysosomal enzymes contribute to the development of many diseases (cancer, neurological disorders, etc.) during inflammation by harming essential macromolecules, which creates a variety of pathological conditions. The anti-inflammatory mechanism prevents the release of lysosomal components that would otherwise harm the tissue and trigger the release of extracellular components, including neutrophils, bactericidal, and fungicidal enzymes.

In the current investigation, ZnO NPs demonstrated impressive, dose-dependent membrane stabilization of HRBCs (Fig. 12). It has been noted that the effect of stabilizing the membrane was enhanced by the increasing concentration of NPs. The stabilizing effects with the standard Diclofenac 85% (20 µg/ mL) and ZnO NPs 84% (100 µg/ mL). The present study observed the ZnO NPs from *Fioria vitifolia* have the greatest inflammatory-reduction action with an IC_{50} value of 60.97 µg/ mL. Thus, green synthesis of zinc oxide nanoparticles from *Fioria vitifolia* has been used as an alternative substitute for the treatment of autoimmune illnesses in the near future and it was supported by [62]. Similarly, [63] reported maximum percentage of anti-inflammatory inhibition (73.01%) was shown in ZnO NPs, and 89.31% inhibition was recorded in *Mussaenda frondosa*-mediated ZnO NPs by [64].

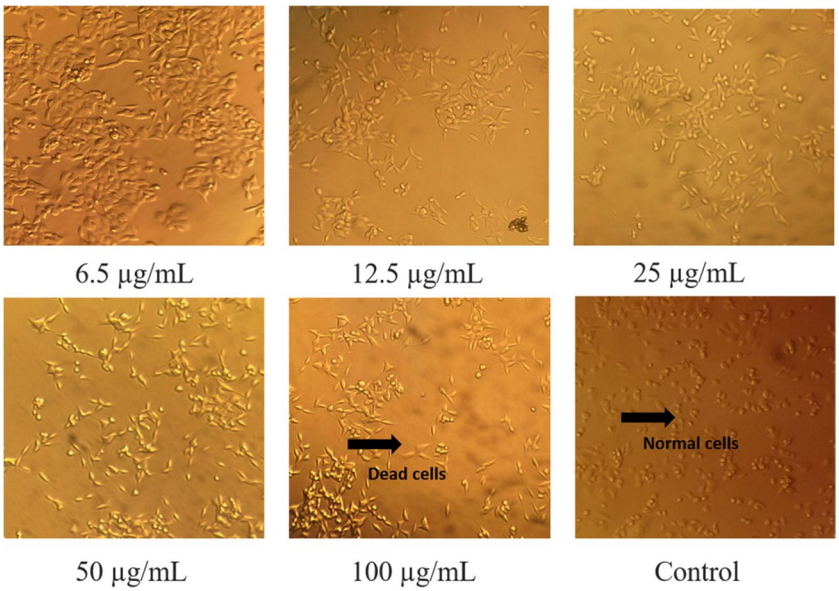

Fig. 14 Anticancer observed at the different concentrations (6.5 µg/ mL, 12.5 µg/ mL, 25 µg/ mL, 50 µg/ mL, 100 µg/ mL, control) of ZnO NPs using *Fioria vitifolia*

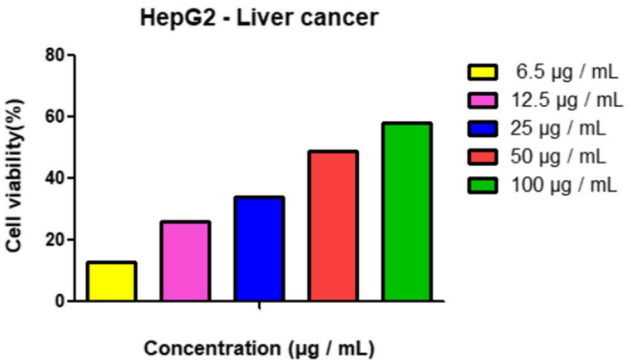

Fig. 15 MTT Assay confirming the anticancer effects of synthesized ZnO NPs by *Fioria vitifolia* against liver cancer cell line (HepG2)

Inhibition of albumin denaturation assay It is generally known that the cause of inflammation resulted in protein denaturation. As part of the inquiry into the biological basis of the inhibiting inflammation, the protein denaturation capability of diluted in series, ZnO NPs was investigated. It was as effective in preventing albumin denaturation brought on by heat. The standard diclofenac drug had an ideal reduction in inhibition of 90% at an average concentration of 15 µg/ mL, whereas ZnO NPs expressed the greatest inhibition of 76% at 400 µg/ mL (Fig. 13). The IC_{50} value of the protein albumin-denatured state for both drugs is 275 µg/ mL and 8.70 µg/ mL, respectively [65]. When [66] examined the beneficial effect on inflammation of ZnO NPs from *Cnidoscolus aconitifolius*, they discovered that 0.35 mg/ mL provided the highest (82.81%) percentage of inhibition [67] revealed that at a concentration of 500 µL, the inflammatory-fighting properties of plant-mediated NPs were 94.62% inhibited.

5.2.4 Using the MTT cytotoxicity test, ZnO NPs *in vitro* anti-cancer efficacy against hepatic malignant cells (HepG2) was assessed

One of the major causes of death globally, cancer is a deadly disease that will probably take the lives of approximately 21 million individuals by the year 2030. Among the various types of cancer, malignancy of the liver currently causes 745, 517 deaths, ranking second among male cancer deaths and sixth among female cancer deaths. The associated risk factors include viral illness, heavy alcohol consumption, and toxin exposure (aflatoxin). The MTT cytotoxicity test was used to assess the synthesized Zinc oxide NPs' capacity to prevent the proliferation of cells associated with liver cancer (HepG2). The major results of the 48-h ZnO NPs treatment of HepG2 cells using a range of doses between 6.5 and 100 µg / mL (Fig. 13) MTT cytotoxicity testing. Data from the current experiment revealed that HepG2 cancer cells' metabolic activity had significantly decreased. The greatest inhibitory potential (57.74% mortality) was noted at 100 µg / mL. As the concentration was lowered, the strength of the cytotoxicity increased. ZnO NPs may have a potential anticancer effect, as evidenced by the decrease in metabolic activity and the result expressed to have an IC_{50} of 52.60 µg/ mL against HepG2 cell lines (Figs. 14 and 15). The harmful effects produced by ZnO NPs at lower concentrations may be due to botanical elements bound to the ZnO NPs, according to [68]. Another study reported the ZnO NPs synthesized from *Pandanus odorifer* extracts from leaves have observed better cytotoxicity effect against the HepG2 cell line, with a 62% inhibition [69]. Recently, [70] investigated ZnO NPs from *Aquilegia*

pubiflora leaf extract showed significant cytotoxic potential properties against cancerous cell lines.

6 Conclusion

To create NPs using green method that protect the environment rather than using hazardous chemical reduction agents and organic solvents, one should make use of recent advancements in nanotechnology. Analyzing, ZnO NPs made from *Fioria vitifolia* leaf extract was the goal of the current work. The biosynthesized ZnO NPs UV–Vis absorbance peak was discernible at 371 nm. The XRD pattern showed the pure hexagonal wurtzite structure. The creation of deep peaks was confirmed by FTIR to be the product of many functional groups. SEM coupled with EDX, and HR-TEM analysis exhibited the spherical structure of synthesized NPs. ZnO NPs have antioxidant properties, as demonstrated by the DPPH and ABTS tests, with an IC_{50} value of 122.37 µg/ mL and 3.07 µg/ mL, respectively, at various dosages. In addition, ZnO NPs showed outstanding curative properties against both Gram-positive (*Bacillus subtilis* and *Staphylococcus aureus*) and Gram-negative (*Klebsiella pneumonia* and *Pseudomonas aeruginosa*) bacterial strains. Similarly, balancing the in vitro tests for albumin denaturation and HRBC membrane stabilization, which both had IC_{50} values of 275 µg/ mL and 60.97 µg/ mL, respectively, revealed ZnO NPs to be more effective as a medication for inflammation. The results of anti-proliferative experiments employing the HepG2 cell line demonstrated a better IC_{50} value of 52.60 µg/ mL for liver cancer. The outcomes of this study show that manufactured ZnO NPs have potent anti-inflammatory, antibacterial, antioxidant, and anticancer effects, making them a suitable replacement for artificial medications in the fields of pharmacological and biological studies.

Supplementary Information The online version contains supplementary material available at https://doi.org/10.1007/s13399-023-04961-9.

Author contribution Raji Meena: investigation, conceptualization, methodology, writing an original draft. Sivakumar Saipraba: investigation, conceptualization, methodology, writing original draft. Devarajan Natarajan: writing original draft. Abdel-Rhman Z. Gaafar and Irshad Arshad: fund provided for the characterization of nanoparticles. Subban Murugesan: conceptualization, methodology, writing an original draft.

Funding This work is supported by the Researchers Supporting Project number RSPD2023R686, King Saud University, Riyadh, Saudi Arabia.

Data availability The data sets used and/or analyzed during the current study are available from the authors upon reasonable request.

Declarations

Ethics approval Not applicable.

Consent to participate Not applicable.

Consent for publication All authors have read the final version of the article and agreed to publish it in Biomass Conversion and Biorefinery.

Competing interests The authors declare no competing interests.

References

1. Khan F, Shariq M, Asif M, Siddiqui MA, Malan P, Ahmad F (2022) Green nanotechnology: plant-mediated nanoparticle synthesis and application. Nanomaterials 12(4):673. https://doi.org/10.3390/nano12040673
2. Hussain I, Singh NB, Singh A et al (2016) Green synthesis of nanoparticles and its potential application. Biotechnol Lett 38:545–560. https://doi.org/10.1007/s10529-015-2026-7
3. Jamdagni P, Khatri P, Rana JS (2018) Green synthesis of zinc oxide nanoparticles using flower extract of Nyctanthes arbor-tristis and their antifungal activity. J King Saud Univ-Sci 30(2):168–175. https://doi.org/10.1016/j.jksus.2016.10.002
4. Mahendiran D, Subash G, Arumai SD et al (2017) Biosynthesis of zinc oxide nanoparticles using plant extracts of Aloe vera and Hibiscus sabdariffa: phytochemical, antibacterial, antioxidant and anti-proliferative studies. BioNanoSci 7:530–545. https://doi.org/10.1007/s12668-017-0418-y
5. Sonia S, Ruckmani K, Sivakumar M (2017) Antimicrobial and antioxidant potentials of biosynthesized colloidal zinc oxide nanoparticles for a fortified cold cream formulation: a potent nanocosmeceutical application. Mater Sci Eng C 79:581–589. https://doi.org/10.1016/j.msec.2017.05.059
6. Seshadri VD (2021) Zinc oxide nanoparticles from Cassia auriculata flowers showed the potent antimicrobial and in vitro anticancer activity against the osteosarcoma MG-63 cells. Saudi J Biol Sci 28(7):4046–4054. https://doi.org/10.1016/j.sjbs.2021.04.001
7. D'Souza JN, Nagaraja GK, Prabhu A, Navada KM, Kouser S, Manasa DJ (2021) Sauropus androgynus (L.) leaf phytochemical activated biocompatible zinc oxide nanoparticles: an antineoplastic agent against human triple negative breast cancer and a potent nanocatalyst for dye degradation. Appl Surf Sci 552:149429. https://doi.org/10.1016/j.apsusc.2021.149429
8. Manimegalai P, Selvam K, Loganathan S et al (2023) Green synthesis of zinc oxide (ZnO) nanoparticles using aqueous leaf extract of Hardwickia binata: their characterizations and biological applications. Biomass Conv Bioref. https://doi.org/10.1007/s13399-023-04279-6
9. Chen H, Yada R (2011) Nanotechnologies in agriculture: new tools for sustainable development. Trends Food Sci Technol 22(11):585–594. https://doi.org/10.1016/j.tifs.2011.09.004
10. Sabir S, Arshad M, Chaudhari SK (2014) Zinc oxide nanoparticles for revolutionizing agriculture: synthesis and applications. Sci World J. https://doi.org/10.1155/2014/925494
11. Mittal D, Kaur G, Singh P, Yadav K, Ali SA (2020) Nanoparticle-based sustainable agriculture and food science: recent advances and future outlook. Front Nanotechnol 2:10. https://doi.org/10.3389/fnano.2020.579954
12. Alrajhi AH, Ahmed NM (2022) Green synthesis of zinc oxide nanoparticles using Salvia officinalis extract. In: Shanker, U., Hussain, C.M., Rani, M. (eds) Handbook of Green and Sustainable Nanotechnology. Springer, Cham. https://doi.org/10.1007/978-3-030-69023-6_44-1

13. Datta A, Patra C, Bharadwaj H, Kaur S, Dimri N et al (2017) Green synthesis of zinc oxide nanoparticles using *Parthenium hysterophorus* leaf extract and evaluation of their antibacterial properties. J Biotechnol Biomater 7:271. https://doi.org/10.4172/2155-952X.1000271
14. Ezealisiji KM, Siwe-Noundou X, Maduelosi B et al (2019) Green synthesis of zinc oxide nanoparticles using *Solanum torvum* (L) leaf extract and evaluation of the toxicological profile of the ZnO nanoparticles–hydrogel composite in Wistar albino rats. Int Nano Lett 9:99–107. https://doi.org/10.1007/s40089-018-0263-1
15. Nayem SA, Shah SS, Chaity SB, Biswas BK, Nahar B, Aziz MA, Hossain MZ (2022) Jute stick extract assisted hydrothermal synthesis of zinc oxide nanoflakes and their enhanced photocatalytic and antibacterial efficacy. Arab J Chem 15(11):104265. https://doi.org/10.1016/j.arabjc.2022.104265
16. Mahalakshmi K, Senthilkumar N, Solairaj P, Parthiban KG (2013) Isolation of triterpenes from Fioria vitifolia (L.) and it's antioxidant activity. Int J Pharm Sci Res 4(9):3596–3600. https://doi.org/10.13040/IJPSR.0975-8232.4(9).3596-00
17. Ramya V, Kalaiselvi V, Kannan SK et al (2022) Facile synthesis and characterization of zinc oxide nanoparticles using Psidium guajava leaf extract and their antibacterial applications. Arab J Sci Eng 47:909–918. https://doi.org/10.1007/s13369-021-05717-1
18. Annapoorani A, Koodalingam A, Beulaja M, Saiprasad G, Chitra P, Stephen A, Manikandan R (2022) Eco-friendly synthesis of zinc oxide nanoparticles using Rivina humilis leaf extract and their biomedical applications. Process Biochem 112:192–202. https://doi.org/10.1016/j.procbio.2021.11.022
19. Vijayakumar S, Vaseeharan B, Sudhakaran R et al (2019) Bioinspired zinc oxide nanoparticles using Lycopersicon esculentum for antimicrobial and anticancer applications. J Clust Sci 30:1465–1479. https://doi.org/10.1007/s10876-019-01590-z
20. Umamaheswari A, Prabu SL, John SA, Puratchikody A (2021) Green synthesis of zinc oxide nanoparticles using leaf extracts of *Raphanus sativus* var. Longipinnatus and evaluation of their anticancer property in A549 cell lines. Biotechnol Rep 29:e00595. https://doi.org/10.1016/j.btre.2021.e00595
21. Nayak A, Sahoo JK, Sahoo SK, Sahu D (2022) Removal of congo red dye from aqueous solution using zinc oxide nanoparticles synthesised from *Ocimum sanctum* (Tulsi leaf): a green approach. Int J Environ Anal Chem 102(19):7889–7910. https://doi.org/10.1080/03067319.2020.1842386
22. Sharma P, Urfan M, Anand R et al (2022) Green synthesis of zinc oxide nanoparticles using *Eucalyptus lanceolata* leaf litter: characterization, antimicrobial and agricultural efficacy in maize. Physiol Mol Biol Plants 28:363–381. https://doi.org/10.1007/s12298-022-01136-0
23. Rahman F, MajedPatwary MA, Bakar Siddique MA, Bashar MS, Haque MA, Akter B, Royhan Uddin AKM (2022) Green synthesis of zinc oxide nanoparticles using *Cocos nucifera* leaf extract: characterization, antimicrobial, antioxidant and photocatalytic activity. R Soc Open Sci 9(11):220858. https://doi.org/10.1098/rsos.220858
24. Kumar R, Bhoj GS, Wohra K, Ali SR, Haider N, Karmakar R (2023) Polymer precursor method for the synthesis of zinc oxide nanoparticles: a novel approach. https://doi.org/10.21203/rs.3.rs-2413923/v1
25. Santhoshkumar J, Kumar SV, Rajeshkumar S (2017) Synthesis of zinc oxide nanoparticles using plant leaf extract against urinary tract infection pathogen. Resour-Efficient Technol 3(4):459–465. https://doi.org/10.1016/j.reffit.2017.05.001
26. Brand-Williams W, Cuvelier M-E, Berset C (1995) Use of a free radical method to evaluate antioxidant activity. LWT-Food Sci Technol 28:25–30. https://doi.org/10.1016/S0023-6438(95)80008-5
27. Re R, Pellegrini N, Proteggente A, Pannala A, Yang M, Rice-Evans C (1999) Antioxidant activity applying an improved ABTS radical cation decolorization assay. Free Radical Biol Med 26:1231–1237. https://doi.org/10.1016/S0891-5849(98)00315-3
28. Gandhidasan R, Thamaraichelvan A, Baburaj S (1991) Anti-inflammatory action of *Lannea coromandelica* by HRBC membrane stabilization. Fitoterapia 62(1):81–83
29. Gunathilake K, Ranaweera K, Rupasinghe HV (2018) In vitro anti-inflammatory properties of selected green leafy vegetables. Biomedicines 6:107. https://doi.org/10.3390/biomedicines6040107
30. Mosmann T (1983) Rapid colorimetric assay for cellular growth and survival: application to proliferation and cytotoxicity assays. J Immunol Methods 65:55–63. https://doi.org/10.1016/0022-1759(83)90303-4
31. Monks A, Scudiero D, Skehan P, Shoemaker R, Paull K, Vistica D, Hose C, Langley J, Cronise P, Vaigro-Wolff A, Gray-Goodrich M, Campbell H, MayoBoyd J (1991) Feasibility of high flux anticancer drug screen using a diverse panel of cultured human tumour cell lines. J Natl Cancer Inst 83:757–766. https://doi.org/10.1093/jnci/83.11.757
32. Vijayakumar S, Krishnakumar C, Arulmozhi P, Mahadevan S, Parameswari N (2018) Biosynthesis, characterization and antimicrobial activities of zinc oxide nanoparticles from leaf extract of *Glycosmis pentaphylla* (Retz.) DC. Microb Pathog 116:44–48. https://doi.org/10.1016/j.micpath.2018.01.003
33. Shwetha UR, Latha MS, Rajith Kumar CR et al (2020) Facile synthesis of zinc oxide nanoparticles using novel *Areca catechu* leaves extract and their in vitro antidiabetic and anticancer studies. J Inorg Organomet Polym 30:4876–4883. https://doi.org/10.1007/s10904-020-01575-w
34. Rajapriya M, Sharmili SA, Baskar R et al (2020) Synthesis and characterization of zinc oxide nanoparticles using *Cynara scolymus* leaves: enhanced hemolytic, antimicrobial, antiproliferative, and photocatalytic activity. J Clust Sci 31:791–801. https://doi.org/10.1007/s10876-019-01686-6
35. Musa I, Qamhieh N (2019) Study of optical energy gap and quantum confinment effects in zinc oxide nanoparticles and nanorods.
36. Chieng BW, Ibrahim NA, Wan Yunus WMZ, Hussein MZ (2013) Poly (lactic acid)/poly (ethylene glycol) polymer nanocomposites: effects of graphene nanoplatelets. Polymers 6(1):93–104
37. Sathappan S, Kirubakaran N, Gunasekaran D et al (2021) Green synthesis of zinc oxide nanoparticles (ZnO NPs) using *Cissus quadrangularis*: characterization, antimicrobial and anticancer studies. Proc Natl Acad Sci India Sect B Biol Sci 91:289–296. https://doi.org/10.1007/s40011-020-01215-w
38. Vijayakumar S, Mahadevan S, Arulmozhi P, Sriram S, Praseetha PK (2018) Green synthesis of zinc oxide nanoparticles using *Atalantia monophylla* leaf extracts: characterization and antimicrobial analysis. Mater Sci Semicond Process 82:39–45. https://doi.org/10.1016/j.mssp.2018.03.017
39. Alahdal FA, Qashqoosh MT, Manea YK, Salem MA, Khan AM, Naqvi S (2022) Eco-friendly synthesis of zinc oxide nanoparticles as nanosensor, nanocatalyst and antioxidant agent using leaf extract of *P*. austroarabica. OpenNano 8:100067. https://doi.org/10.1016/j.onano.2022.100067
40. Varadavenkatesan T, Lyubchik E, Pai S, Pugazhendhi A, Vinayagam R, Selvaraj R (2019) Photocatalytic degradation of Rhodamine B by zinc oxide nanoparticles synthesized using the leaf extract of *Cyanometra ramiflora*. J Photochem Photobiol B 199:111621. https://doi.org/10.1016/j.jphotobiol.2019.111621
41. Ogunyemi SO, Abdallah Y, Zhang M, Fouad H, Hong X, Ibrahim E, ... & Li B (2019) Green synthesis of zinc oxide

nanoparticles using different plant extracts and their antibacterial activity against *Xanthomonas oryzae* pv. oryzae. Artif Cells Nanomed Biotechnol 47(1):341–352. https://doi.org/10.1080/21691401.2018.1557671

42. Hou Y, Hou Y, Ren Y, Shi Y, Jin X, Dong Y, Zhang H (2020) *C. aromaticus* leaf extract mediated synthesis of zinc oxide nanoparticles and their antimicrobial activity towards clinically multidrug-resistant bacteria isolated from pneumonia patients in nursing care. Mater Res Express 7(9):095015. https://doi.org/10.1088/2053-1591/abb427
43. Aminuzzaman M, Ying LP, Goh WS et al (2018) Green synthesis of zinc oxide nanoparticles using aqueous extract of *Garcinia mangostana* fruit pericarp and their photocatalytic activity. Bull Mater Sci 41:50. https://doi.org/10.1007/s12034-018-1568-4
44. Mahendra C, Murali M, Manasa G et al (2017) Antibacterial and antimitotic potential of bio-fabricated zinc oxide nanoparticles of Cochlospermum religiosum (L.). Microb Pathog 110:620–629. https://doi.org/10.1016/j.micpath.2017.07.051
45. Muhammad W, Ullah N, Haroon M et al (2019) Optical, morphological and biological analysis of zinc oxide nanoparticles (ZnO NPs) using Papaver somniferum L. RSC Adv 9(51):29541–29548. https://doi.org/10.1039/C9RA04424H
46. Suntako R (2015) Effect of zinc oxide nanoparticles synthesized by a precipitation method on mechanical and morphological properties of the CR foam. Bull Mater Sci 38:1033–1038. https://doi.org/10.1007/s12034-015-0921-0
47. Arumugam M, Manikandan DB, Dhandapani E, Sridhar A, Balakrishnan K, Markandan M, Ramasamy T (2021) Green synthesis of zinc oxide nanoparticles (ZnO NPs) using *Syzygium cumini*: potential multifaceted applications on antioxidants, cytotoxic and as nanonutrient for the growth of *Sesamum indicum*. Environ Technol Innov 23:101653. https://doi.org/10.1016/j.eti.2021.101653
48. Ramesh P, Saravanan K, Manogar P, Johnson J, Vinoth E, Mayakannan M (2021) Green synthesis and characterization of biocompatible zinc oxide nanoparticles and evaluation of its antibacterial potential. Sens Bio-Sens Res 31:100399. https://doi.org/10.1016/j.sbsr.2021.100399
49. Al-Kordy HM, Sabry SA, Mabrouk ME (2021) Statistical optimization of experimental parameters for extracellular synthesis of zinc oxide nanoparticles by a novel haloalaliphilic Alkalibacillus sp. W7. Sci Rep 11(1):1–14
50. Chen L, Batjikh I, Hurh J, Han Y, Huo Y, Ali H, ... & Yang D. C (2019) Green synthesis of zinc oxide nanoparticles from root extract of *Scutellaria baicalensis* and its photocatalytic degradation activity using methylene blue. Optik 184:324–329. https://doi.org/10.1016/j.ijleo.2019.03.051
51. Bhosale AS, Abitkar KK, Sadalage PS, Pawar KD, Garadkar KM (2021) Photocatalytic and antibacterial activities of ZnO nanoparticles synthesized by chemical method. J Mater Sci Mater Electron 32:20510–20524
52. Sukri SNAM, Shameli K, Wong MMT, Teow SY, Chew J, Ismail NA (2019) Cytotoxicity and antibacterial activities of plant-mediated synthesized zinc oxide (ZnO) nanoparticles using *Punica granatum* (pomegranate) fruit peels extract. J Mol Struct 1189:57–65. https://doi.org/10.1016/j.molstruc.2019.04.026
53. Bharathi D, Bhuvaneshwari V (2019) Synthesis of zinc oxide nanoparticles (ZnO NPs) using pure bioflavonoid rutin and their biomedical applications: antibacterial, antioxidant and cytotoxic activities. Res Chem Intermed 45:2065–2078. https://doi.org/10.1007/s11164-018-03717-9
54. Sepasgozar SME, Mohseni S, Feizyzadeh B et al (2021) Green synthesis of zinc oxide and copper oxide nanoparticles using *Achillea nobilis* extract and evaluating their antioxidant and antibacterial properties. Bull Mater Sci 44:129. https://doi.org/10.1007/s12034-021-02419-0
55. Ravichandran V, Sumitha S, Ning CY, Xian OY, Kiew Yu U, Paliwal N, ... & Tripathy M (2020) Durian waste mediated green synthesis of zinc oxide nanoparticles and evaluation of their antibacterial, antioxidant, cytotoxicity and photocatalytic activity. Green Chem Lett Rev 13(2):102–116. https://doi.org/10.1080/17518253.2020.1738562
56. Chandra H, Patel D, Kumari P, Jangwan JS, Yadav S (2019) Phyto-mediated synthesis of zinc oxide nanoparticles of *Berberis aristata*: characterization, antioxidant activity and antibacterial activity with special reference to urinary tract pathogens. Mater Sci Eng C 102:212–220. https://doi.org/10.1016/j.msec.2019.04.035
57. Ananthalakshmi R, Rajarathinam SR, Sadiq AM (2019) Antioxidant activity of ZnO nanoparticles synthesized using *Luffa acutangula* peel extract. Res J Pharm Technol 12(4):1569–1572. https://doi.org/10.5958/0974-360X.2019.00260.9
58. Safawo T, Sandeep BV, Pola S, Tadesse A (2018) Synthesis and characterization of zinc oxide nanoparticles using tuber extract of anchote (*Coccinia abyssinica* (Lam.) Cong.) for antimicrobial and antioxidant activity assessment. OpenNano 3:56–63. https://doi.org/10.1016/j.onano.2018.08.001
59. Krishnan BR, Ramesh M, Selvakumar M et al (2020) A facile green approach of cone-like ZnO NSs synthesized via *Jatropha gossypifolia* leaves extract for photocatalytic and biological activity. J Inorg Organomet Polym 30:4441–4451. https://doi.org/10.1007/s10904-020-01576-9
60. Faisal S, Jan H, Shah SA, Shah S, Khan A, Akbar MT, Syed S (2021) Green synthesis of zinc oxide (ZnO) nanoparticles using aqueous fruit extracts of *Myristica fragrans*: their characterizations and biological and environmental applications. ACS Omega 6(14):9709–9722. https://doi.org/10.1021/acsomega.1c00310
61. Sanaeimehr Z, Javadi I, Namvar F (2018) Antiangiogenic and antiapoptotic effects of green-synthesized zinc oxide nanoparticles using *Sargassum muticum* algae extraction. Cancer Nano 9:3. https://doi.org/10.1186/s12645-018-0037-5
62 Manasa DJ, Chandrashekar KR, Kumar MP, Suresh D, Kumar DM, Ravikumar CR, Murthy HA (2021) Proficient synthesis of zinc oxide nanoparticles from *Tabernaemontana heyneana* Wall. via green combustion method: antioxidant, anti-inflammatory, antidiabetic, anticancer and photocatalytic activities. Results Chem 3:100178. https://doi.org/10.1016/j.rechem.2021.100178
63. Zahoor S, Sheraz S, Shams DF, Rehman G, Nayab S, Shah MIA, Khan W (2023) Biosynthesis and anti-inflammatory activity of zinc oxide nanoparticles using leaf extract of *Senecio chrysanthemoides*. Biomed Res Int. https://doi.org/10.1155/2023/3280708
64. Jayappa MD, Ramaiah CK, Kumar MAP et al (2020) Green synthesis of zinc oxide nanoparticles from the leaf, stem and in vitro grown callus of *Mussaenda frondosa* L.: characterization and their applications. Appl Nanosci 10:3057–3074. https://doi.org/10.1007/s13204-020-01382-2
65. Vijayakumar N, Bhuvaneshwari VK, Ayyadurai GK, Jayaprakash R, Gopinath K, Nicoletti M, Govindarajan M (2022) Green synthesis of zinc oxide nanoparticles using *Anoectochilus elatus*, and their biomedical applications. Saudi J Biol Sci 29(4):2270–2279. https://doi.org/10.1016/j.sjbs.2021.11.065
66. Dangana RS, George RC, Agboola FK (2023) The biosynthesis of zinc oxide nanoparticles using aqueous leaf extracts of *Cnidoscolus aconitifolius* and their biological activities. Green Chem Lett Rev 16(1):2169591. https://doi.org/10.1080/17518253.2023.2169591

67. Sanjivkumar M, Silambarasan T, Ananthi S et al (2022) Biosynthesis and characterization of zinc oxide nanoparticles from an estuarine-associated actinobacterium *Streptomyces spp*. and its biotherapeutic applications. Arch Microbiol 204:17. https://doi.org/10.1007/s00203-021-02609-8
68. Abbasi BA, Iqbal J, Ahmad R, Zia L, Kanwal S, Mahmood T, Chen JT (2019) Bioactivities of *Geranium wallichianum* leaf extracts conjugated with zinc oxide nanoparticles. Biomolecules 10(1):38. https://doi.org/10.3390/biom10010038
69. Hussain A, Oves M, Alajmi MF, Hussain I, Amir S, Ahmed J, Ali I (2019) Biogenesis of ZnO nanoparticles using *Pandanus odorifer* leaf extract: anticancer and antimicrobial activities. RSC Adv 9(27):15357–15369. https://doi.org/10.1039/C9RA01659G
70. Jan H, Shah M, Andleeb A, Faisal S, Khattak A, Rizwan M, Abbasi BH (2021) Plant-based synthesis of zinc oxide nanoparticles (ZnO-NPs) using aqueous leaf extract of *Aquilegia pubiflora*: their antiproliferative activity against HepG2 cells inducing reactive oxygen species and other in vitro properties. Oxid Med Cell Longev. https://doi.org/10.1155/2021/4786227